J. Biochem. **139**, 213–221 (2006)
doi:10.1093/jb/mvj027

Binding of Glucose to the D-Galactose/D-Glucose–Binding Protein from *Escherichia coli* Restores the Native Protein Secondary Structure and Thermostability That Are Lost upon Calcium Depletion

Sabato D'Auria[1,*], Alessio Ausili[2], Anna Marabotti[3,4], Antonio Varriale[1], Viviana Scognamiglio[1], Maria Staiano[1], Enrico Bertoli[2], Mosè Rossi[1] and Fabio Tanfani[2]

[1]Istituto di Biochimica delle Proteine, CNR, Via P. Castellino, 111 80131 Napoli, Italy; [2]Istituto di Biochimica, Università Politecnica delle Marche, Via Ranieri, 60131 Ancona, Italy; [3]Laboratorio di Bioinformatica, Istituto di Scienze dell'Alimentazione, CNR, via Roma 52 A/C, 83100 Avellino, Italy; and [4]Centro di Ricerca Interdipartimentale di Scienze Computazionali e Biotecnologiche (CRISCEB), Seconda Universitá degli Studi di Napoli, Via Costantinopoli, 16, 80138 Napoli, Italy

Received September 20, 2005; accepted October 28, 2005

The effect of the depletion of calcium on the structure and thermal stability of the D-galactose/D-glucose–binding protein (GGBP) from *Escherichia coli* was studied by fluorescence spectroscopy and Fourier-transform infrared spectroscopy. The calcium-depleted protein (GGBP-Ca) was also studied in the presence of glucose (GGBP-Ca/Glc). The results show that calcium depletion has a small effect on the secondary structure of GGBP, and, in particular it affects a population of α-helices with a low exposure to solvent. Alternatively, glucose-binding to GGBP-Ca eliminates the effect induced by calcium depletion by restoring a secondary structure similar to that of the native protein. In addition, the infrared and fluorescence data obtained reveal that calcium depletion markedly reduces the thermal stability of GGBP. In particular, the spectroscopic experiments show that the depletion of calcium mainly affects the stability of the C-terminal domain of the protein. However, the binding of glucose restores the thermal stability of GGBP-Ca. The thermostability of GGBP and GGBP-Ca was also studied by molecular dynamics simulations. The simulation data support the spectroscopic results. New insights into the role of calcium in the thermal stability of GGBP contribute to a better understanding of the protein function and constitute important information for the development of biotechnological applications of this protein. Mutations and/or labelling of amino acid residues located in the protein C-terminal domain may affect the stability of the whole protein structure.

Key words: galactose/glucose-binding protein, infrared spectroscopy, protein stability, protein structure.

Abbreviations: GGBP, native D-galactose/D-glucose binding protein; GGBP/Glc, GGBP in the presence of 10 mM glucose; GGBP-Ca, Calcium-depleted GGBP; GGBP-Ca/Glc, GGBP-Ca in the presence of 10 mM glucose; FT-IR, Fourier transform infrared; Amide I′, amide I band in ^2H_2O medium.

Protein folding and stability investigations are topics of tremendous intellectual interest since they contribute to completing the information transfer from DNA to active protein products (*1*). In addition, the fundamental principles of protein stability also have practical applications in the understanding of different pathologies, in the design of novel proteins with special features, and in the industrial exploitation of recent advances in biotechnology and applied enzymology (*2*).

D-Galactose/D-glucose binding protein (GGBP) is a bacterial periplasmic protein, an initial component for both chemotaxis towards galactose and glucose and active transport of the two sugars. Several well-refined structures of the GGBP from *Escherichia coli* and *Salmonella typhimurium* in the absence and in the presence of sugars have been obtained by X-ray crystallography (*3–7*). The example in Fig. 1A represents the X-ray structure of GGBP from *S. typhimurium* solved at 1.9 Å (*5*). This protein is a monomer with a molecular mass of about 32 kDa, with a structure organized into two main domains linked by three strands commonly referred to as the hinge region. Glucose and galactose bind with micromolar affinity to GGBP in the groove between the two domains, and conformational changes involving the hinge are necessary for the sugars to enter and exit the protein binding site (*8*). In addition, GGBP can also bind other monosaccharides (L-arabinose, L-xylose) with affinity constant 100- to 1,000-fold weaker than glucose. However, since human blood does not contain galactose, arabinose or xylose, it is possible to use GGBP as a probe for glucose detection in the blood (*9*). In fact, several research labs are studying the biotechnological applications of GGBP as a fluorescence probe for advanced biosensors for monitoring the glucose levels of diabetic patients (*10–12*).

*To whom correspondence should be addressed. Tel: +39-0816132250, Fax: +39-0816132277; E-mail: s.dauria@ibp.cnr.it

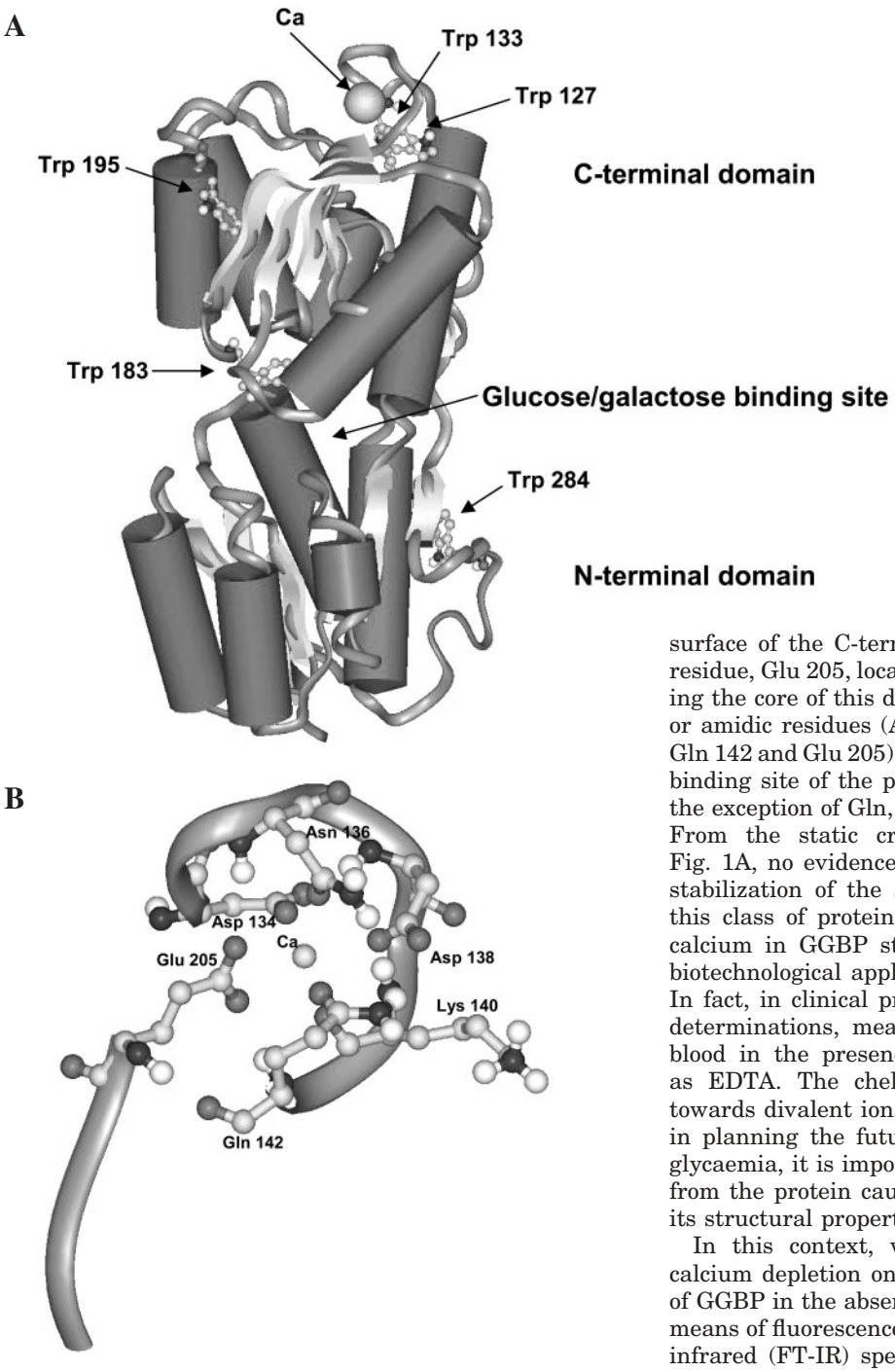

Fig. 1. **Three-dimensional structure of GGBP from *S.*** typhimurium. (a) Crystallographic structure of the whole protein. The picture was obtained from PDB file 1GCG. The N- and C-terminal domains are labelled. Helices are represented as cylinders and β-sheets as arrows. The Ca^{2+} ion is represented as a ball and the tryptophan residues are shown in ball & stick mode and labelled. The sugar binding site is localized in the groove between the two domains indicated by the arrow. (b) Close-up of the Ca^{2+}-binding site. The metal ion is represented as the ball, and the residues that coordinate it are represented in ball & stick mode.

Calcium is involved in various biological processes, and one major role of Ca^{2+} is to stabilize the native folds of proteins. For this reason Ca^{2+} is a constituent of many thermostable proteins (*13*). The refined crystallographic structures of GGBP revealed the presence of a Ca^{2+}-binding site located about 30 Å from the sugar binding site. The Ca^{2+}-binding site of the protein from *S. typhimurium* is shown in detail in Fig. 1b. It is formed essentially by a loop (residues 134–142) found at the surface of the C-terminal domain, plus another isolated residue, Glu 205, located near one of the β-strands composing the core of this domain. Only oxygen atoms from acid or amidic residues (Asp 134, Asn 136, Asp 138, Lys 140, Gln 142 and Glu 205) coordinate the metal ion (*3*). The Ca^{2+} binding site of the protein from *E. coli* is identical, with the exception of Gln, instead of Lys, in position 140 (*3*, *4*). From the static crystallographic structure shown in Fig. 1A, no evidence is present for a role of Ca^{2+} in the stabilization of the secondary and tertiary structure of this class of protein. However, the study of the role of calcium in GGBP stability is of tremendous interest if biotechnological applications of this protein are planned. In fact, in clinical practice, in order to speed-up glucose determinations, measurements are performed on whole blood in the presence of an anti-coagulant agent such as EDTA. The chelating properties of this compound towards divalent ions are well known. As a consequence, in planning the future use of GGBP as a biosensor for glycaemia, it is important to know how calcium depletion from the protein caused by chelating agents could affect its structural properties.

In this context, we have investigated the effect of calcium depletion on the structure and thermal stability of GGBP in the absence and in the presence of glucose by means of fluorescence spectroscopy and Fourier transform infrared (FT-IR) spectroscopy in the temperature range of 10–95°C, and by computational dynamics simulations. Our results indicate that even though calcium depletion has only a slight effect on the secondary structure of GGBP by abolishing a part of the α-helical structures with a low exposure to solvent, it does have a marked effect on the thermal stability of the protein. The binding of glucose to the calcium-depleted GGBP restores the protein secondary structure content and its thermostability.

MATERIALS AND METHODS

Materials—Deuterium oxide (99.9 % ^2H_2O), ^2HCl and NaO^2H were purchased from Aldrich. Hepes and D-glucose

were obtained from Sigma. All the other chemicals used were commercial samples of the purest quality.

Preparation and Purification of GGBP and of GGBP-Ca—D-Galactose/D-glucose binding protein (GGBP) from *E. coli* was prepared and purified according to Ref. *14*. Calcium-depleted GGBP (GGBP-Ca) was obtained by extensive dialysis of GGBP against 5.0 mM Tris/HCl, 5.0 mM EDTA buffer pH 8.0 at 4°C. The content of calcium in the GGBP structure was checked by atomic absorption spectroscopy and was found to be negligible after treatment of GGBP with EDTA (*15*). GGBP and GGBP-Ca were stored at 4°C in 5.0 mM Tris/HCl, pH 8.0 and 5.0 mM Tris/HCl, 5.0 mM EDTA buffer, pH 8.0, respectively.

Protein Assay—The protein concentration was determined by the method of Bradford (*16*) with bovine serum albumin as a standard using a double beam Cary 1E spectrophotometer (Varian, Mulgrade, Victoria, Australia).

Fluorescence Spectroscopy—Steady state fluorescence measurements were performed on a K2 fluorometer (ISS, Champaign, IL, USA) equipped with a 2-cell temperature controlled sample holder. In order to avoid the Tyr contribution, the protein sample was excited at 295 nm with a slit width of 1.0 nm. The temperature of the samples was measured directly in the cuvette with an accuracy of ±0.2°C.

Preparation of Samples for Infrared Measurements—The protein samples for infrared spectroscopy were prepared using the following buffers at p^2H 7.0: 25 mM Hepes/NaO^2H (buffer A); 25 mM Hepes/NaO^2H, 10 mM glucose (buffer B); 25 mM Hepes/NaO^2H, 1 mM EDTA (buffer C); 25 mM Hepes, 1 mM EDTA, 10 mM glucose (buffer D). Buffer (A) and (B) were used for GGBP, while buffers (C) and (D) were used for GGBP-Ca. The p^2H values correspond to the pH meter reading +0.4 (*17*). About 1.5 mg of protein, dissolved in the buffer used for its purification, were centrifuged in a "10 K Centricon" micro concentrator (Amicon) at 3,000 × *g* at 4°C, and concentrated to a volume of approximately 30 μl. Then, 250 μl of buffer (A) or (B) or (C) or (D) was added, and the sample was concentrated again. The washings were repeated several times in order to completely replace the original buffer with the buffer used in a particular experiment. In the last washing the protein samples were concentrated to a final volume of approximately 35 μl and used for infrared measurements.

Infrared Spectra—Infrared spectra at 2 cm^{-1} resolution were obtained by means of a Perkin-Elmer 1760-x Fourier transform infrared spectrometer as described (*18*). In the thermal denaturation experiments, the temperature was raised in 5°C steps from 20°C to 95°C using an external bath circulator (HAAKE F3). The actual temperature in the cell was controlled by a thermocouple placed directly onto the window. Spectra were collected and processed using the SPECTRUM software from Perkin-Elmer. Second derivative spectra were calculated over a 9-data-point range (9 cm^{-1}). The midpoint transition (T_m) in the thermal denaturation curves was calculated by fitting the curves to a sigmoid function as described (*19*).

Molecular Dynamics Simulation—The program Insight II (version 2000.1, 2000; Accelrys) was used throughout the calculations. The file 1GCG (*5*) available from Protein Data Bank (*20*) was used as a starting point and managed before molecular dynamics simulations in order to add hydrogen atoms to the carbon atoms (hydrogen atoms bound to non-carbon atoms including water oxygen atoms were already present in the original file) and to set correctly the potentials and the charges of all atoms. After these modifications, this file was considered suitable to simulate the starting structure of GGBP. To simulate the starting structure of GGBP-Ca, the Ca^{2+} atom was deleted from the file and the protein was subjected to mild optimization with 500 minimization steps using the Steepest Descent method, until a final gradient of 0.5 kcal/mol Å. Molecular dynamics simulations were applied with the NVT (constant volume and temperature) ensemble, setting the temperature at 65°C, for a total run of 500 ps (0.5 ns). Snapshots of the system were registered every 1 ps. After about 60 ps of simulation, the calcium was also lost from the binding site of GGBP, and, therefore the comparison of structural features of the two systems was limited to the first 50 ps of simulation. To do this, two molecules representing the "mean" conformation of the proteins during the 50 ps dynamics run were created for both systems by "averaging" all the conformations obtained in the first 50 ps with the aid of Insight II facilities. The program DSSP (*21*) was then used to determine the relative position of secondary structural elements in both the original file and in the results of the dynamics run.

RESULTS AND DISCUSSION

Secondary Structures of GGBP, GGBP-Ca and GGBP-Ca/Glc—Figure 2 shows the resolution-enhanced spectra of GGBP, GGPB-Ca and GGBP-Ca/Glc. The secondary structure of GGBP (Panel A, continuous line) was previously characterized (*18*). Besides other secondary structural elements, it consists of two populations of α-helices belonging to the 1,658 and 1,650.5 cm^{-1} bands (Fig. 2) (*22*). The two populations may differ in their exposure to the solvent (^2H_2O) or in the regularity of folding (distortion) (*23*). The 1,697.2, 1,636.5 and 1,627 cm^{-1} bands are due to β-sheets; and this multiplicity may reflect differences in the hydrogen bonding strength as well as differences in transition dipole coupling in different β-strands (*24*). In particular, the 1,627 cm^{-1} band may be due to β-strands particularly exposed to the solvent, *i.e.* to β-strands at the edge of β-sheet (termed β-edge) that are not hydrogen bonded to another polypeptide extended chain but to a different intra- or intermolecular structure (*22*, *25*) or to unusually strongly hydrogen bonded β-sheet (*26*). The 1,663 cm^{-1} shoulder reveals turns, whilst the 1,674 and 1,681 cm^{-1} bands may be due to turns and/or β sheet (*27*). The 1,582.2 cm^{-1} band is due to ionized carboxyl group of aspartic acids and the 1,515.3 cm^{-1} band is characteristic of the tyrosine residue (*28*, *29*). The band close to 1,550 cm^{-1} represents the residual amide II band, *i.e.* the amide II band (1,600–1,500 cm^{-1} range) after $^1H/^2H$ exchange of the amide hydrogens of the polypeptide chain (*18*).

Comparison of the GGBP and GGBP-Ca spectra (Fig. 2A) reveals small differences in the band position and intensity of the α-helix and β-sheet bands, suggesting that calcium depletion slightly affects the secondary structure of the protein. In particular, the 1,658 cm^{-1} band is not visible in the GGBP-Ca sample suggesting that calcium depletion particularly affects this population

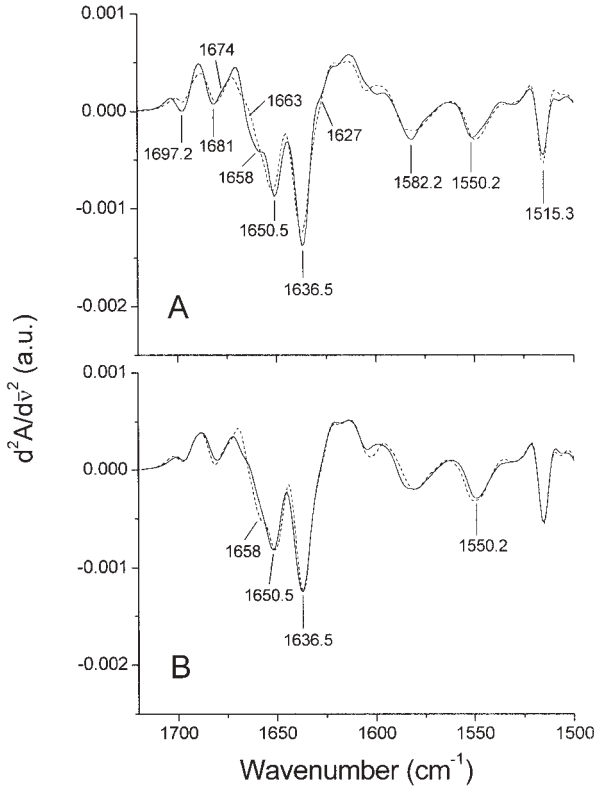

Fig. 2. **Comparison of GGBP, GGBP-Ca, and GGBP-Ca/Glc second derivative infrared spectra at 20°C.** Panel (A): continuous and dashed lines refer to the spectra of GGBP and GGBP-Ca, respectively. Panel (B): continuous and dashed lines refer to the spectra of GGBP-Ca and GGBP-Ca/Glc, respectively.

of α-helices. This band is probably due to α-helices less exposed to the solvent. Indeed, in ^1H_2O medium the absorption of α-helices is indistinguishable from the unordered structures, both absorptions occurring at about 1,658 cm^{-1} (*22*). In ^2H_2O medium the absorption of unordered structures occurs at about 1,645 cm^{-1} while the absorption of α-helices is found between 1,658 and 1,650 cm^{-1}. The extent of the downshift in wavenumber is proportional to the extent of $^1H/^2H$ exchange occurring in the α-helix, *i.e.* to the exposure to the solvent of the secondary structural element. In the GGBP-Ca spectrum, the absence of the 1,658 cm^{-1} band could be due to a more relaxed tertiary structure of the protein allowing enhanced molecular dynamics, and thus a more deep contact of the solvent (^2H_2O) with the polypeptide chains. Indeed, the thermostability of GGBP-Ca is much lower than that of GGBP (see below) supporting the hypothesis of a more relaxed protein structure.

Figure 2B compares the second derivative spectra of GGBP-Ca and GGBP-Ca/Glc. Binding of glucose to GGBP-Ca induces changes in the infrared spectrum of the protein. In particular, it is evident that in the presence of glucose the 1,658 cm^{-1} band, present in the GGBP spectrum, is restored. This phenomenon might be due to a reduced solvent accessibility induced by the interaction of glucose with polypeptide sequences adopting an α-helical structure (*18*) and/or by a protein conformational change involving the hinge region (*8*).

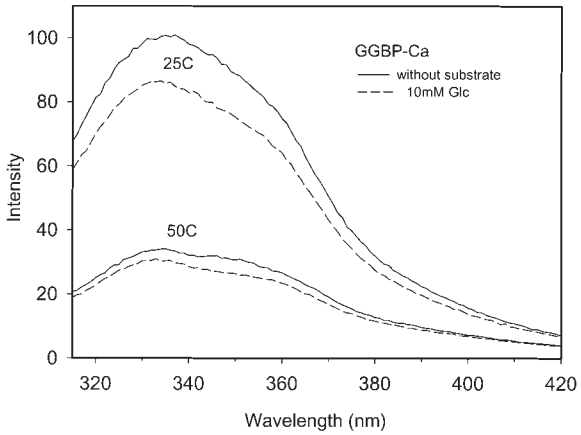

Fig. 3. **Fluorescence spectra of GGBP-Ca in the absence and in the presence of 10 mM glucose at 25 and 50°C.**

Table 1. **Thermal denaturation of GGBP-Ca, GGBP-Ca/Glc GGBP, and GGBP/Glc monitored by fluorescence spectroscopy.**

Protein sample	T_m (°C)
GGBP	48.8
GGBP/Glc	61.4
GGBP-Ca	44.1
GGBP-Ca/Glc	53.2

Thermal Stability—Fluorescence spectroscopy on GGBP, GGBP-Ca and GGBP-Ca/Glc: From the analysis of the protein crystallographic data it appears that four out of the five GGBP tryptophan residues, namely Trp 127, Trp 133, Trp 183, and Trp 195, are located in the C-terminal domain of the protein. The fifth residue, Trp 284, is located in a C-terminal loop headed toward the N-terminal domain (*3*). In addition, the Ca^{2+}-binding site is also located in the C-terminal domain in the close vicinity of Trp 133 and Trp 127 (Fig. 1A). As a consequence, it is evident that the tryptophan fluorescence of the protein predominantly reflects conformational changes in the C-terminal domain and can be informative on the role of calcium in the structure of GGBP.

Figure 3 shows the fluorescence spectra of GGBP-Ca in the absence and presence of glucose at 25 and 50°C. At both temperatures, GGBP-Ca exhibits a broad emission spectrum with a similar spectral shape in the presence and absence of Glc. In the absence of Glc the emission peak is located near 336 nm. The fluorescence maximum of the GGBP-Ca/Glc complex exhibits a minor blue shift with an emission maximum centered near 334 nm. The binding of glucose results in fluorescence quenching at both temperatures. Since Trp 183 is in close vicinity to the glucose-binding site, a part of the quenching may be due to the interaction of Glc with Trp 183. Table 1 shows the melting temperatures of GGBP, GGBP/Glc, GGBP-Ca, and GGBP-Ca/Glc.

It appears that in both the absence and presence of glucose the depletion of the calcium ion from the protein structure results in a significant decrease in the protein melting temperature (T_m). However the binding of glucose to GGBP-Ca restores the protein stability, since the protein T_m increases by about 10°C, from 44.1°C to

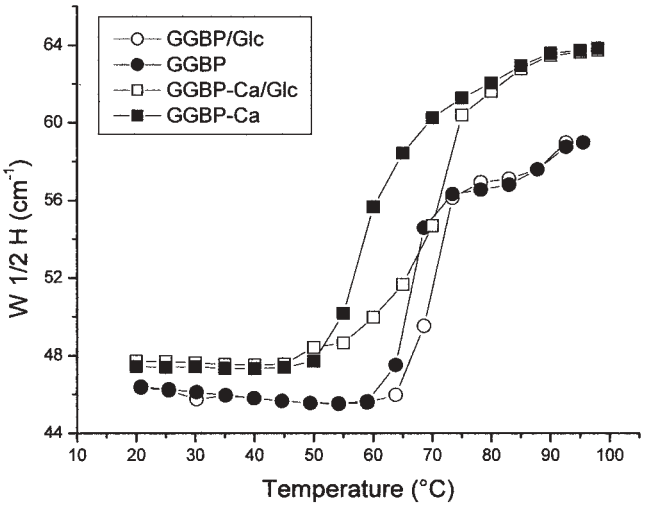

Fig. 4. **Thermal stability of GGBP, GGBP/Glc, GGBP-Ca and GGBP-Ca/Glc.** The thermal stability of the protein was followed by monitoring the amide I′ bandwidth as a function of temperature. The bandwidth was calculated at 1/2 of the amide I′ band height (W1/2H).

53.2°C. The fluorescence data strongly suggest that the removal of calcium severely destabilizes the C-terminal domain of GGBP.

Infrared experiments on GGBP, GGBP/Glc, GGBP-Ca and GGBP-Ca/Glc: Thermal denaturation of the protein was followed by monitoring the amide I′ bandwidth as a function of temperature (*30*, *31*). Although the Ca^{2+} binds to a surface loop that should be quite flexible (as shown in Fig. 1A), calcium depletion destabilizes the protein markedly against high temperatures (Fig. 4). On the other hand the binding of glucose to GGBP-Ca or to GGBP increases the thermostability of the proteins. In particular, the melting temperatures (T_m) were found to be 66.9, 70.2, 60.9 and 70.2°C for GGBP, GGBP/Glc, GGBP-Ca and GGBP-Ca/Glc, respectively. These data indicate that the stabilization of the structure caused by glucose binding exceeds the destabilization induced by calcium depletion since the T_m of GGBP/Glc and of GGBP-Ca/Glc are the same.

The apparent disagreement in the T_m values obtained from the fluorescence and FT-IR experiments may be due to the fact that the changes in Trp fluorescence as a function of increasing temperature reflect predominantly conformational changes in the GGBP C-terminal domain, while the FT-IR data refer to the whole protein structure. In addition, this apparent discrepancy between the fluorescence and FT-IR data can be explained by the very low protein concentration used in the fluorescence experiments (0.05 mg/ml) compared to the FT-IR experiments (30 mg/ml). Moreover, the difference in the two sets of data indicates that the unfolding of the C-terminal domain of GGBP occurs at a lower T_m value than that of the N-terminal domain.

It should be pointed out that the T_m values reported in the present work differ from those reported by Piszczek *et al.* (*15*). These differences may be attributed to the different protein concentrations used in the experiments reported in the two works. In fact, we already described the different thermal behavior of the beta-glycosidase isolated from the thermophilic archaeon *Sulfolobus solfataricus* as investigated by different techniques (circular dichroism, differential scanning calorimetry, FT-IR), each of which requires a different protein concentration (*32*).

The thermal destabilization induced by calcium depletion and the stabilization induced by glucose binding to GGBP or to GGBP-Ca can be observed also by monitoring the intensity of the α-helix and β-sheet bands as a function of temperature (Fig. 5). The figure shows that the α-helix, the β-sheet, and the residual amide II bands decrease in intensity with an increase in temperature. Moreover, the increase in temperature leads to the formation of two new bands at 1,617 and 1,682 cm^{-1} due to intermolecular interactions (aggregation) brought about by protein thermal denaturation (*18*, *33*, *34*). The large decrease in the intensities of the α-helix and the β-sheet bands reflects the thermal denaturation of the corresponding structural elements.

In particular, the spectra of GGBP and GGBP/Glc show that the 1,658 cm^{-1} band (α-helix poorly exposed to solvent) and the 1,627 cm^{-1} shoulder (β-strand) are particularly sensitive to temperature since the intensities of these bands decrease at relatively low temperatures as compared with the other α-helix (1,650.5 cm^{-1}) and β-sheet (1,636.5 cm^{-1}) bands. Indeed, the 1,658 cm^{-1} band disappears from the spectra of GGBP and GGBP/Glc at 50 and 55°C, respectively. The 1,627 cm^{-1} band is hardly visible above 40°C in either the GGBP or GGBP/Glc spectrum. As Fig. 2 shows, glucose binding to GGBP-Ca restores the 1,658 cm^{-1} band to the spectrum of the protein. This band is also particularly temperature-sensitive since it disappears at between 55–60°C. Analysis of the spectra reported in Fig. 5 also reveals that the disappearance of secondary structural element bands occurs at 70, 75, 65, and 75°C for GGBP, GGBP/Glc, GGBP-Ca and GGBP-Ca/Glc, respectively. At, and above the reported temperatures, the spectra are characterized by a broad band centred at 1,644 cm^{-1} (unordered structures) and by the two bands close to 1,617 and 1,682 cm^{-1} that are characteristic of protein intermolecular interactions (aggregation). Figure 6 shows the temperature-dependent decrease in the intensity of the main α-helix and β-sheet bands. In particular, panel A shows that, with the increase in temperature, the α-helix band intensity of the spectra of the different protein samples remains almost constant, and then, at a particular temperature, the band intensity decreases suddenly. The onset of thermal denaturation of the structural element can be estimated from the graphs. The onset of α-helix denaturation for GGBP, GGBP/Glc, GGBP-Ca, and GGBP-Ca/Glc is 60, 65, 50°C, and about 65–70°C, respectively. Table I reports the onset of α-helix and β-sheet thermal denaturation and the corresponding T_m values. It is worth nothing that the thermal stability of the α-helices in GGBP-Ca/Glc is similar to that of α-helices in GGBP/Glc. Likewise, the thermal stability of the β-sheets (Fig. 6B and Table 2) is similar in GGBP-Ca/Glc and in GGBP/Glc, whilst in GGBP-Ca it is lower.

The data reported in Table 2 indicate that the main α-helix and the main β-sheet populations present in the different protein samples have similar thermal stabilities

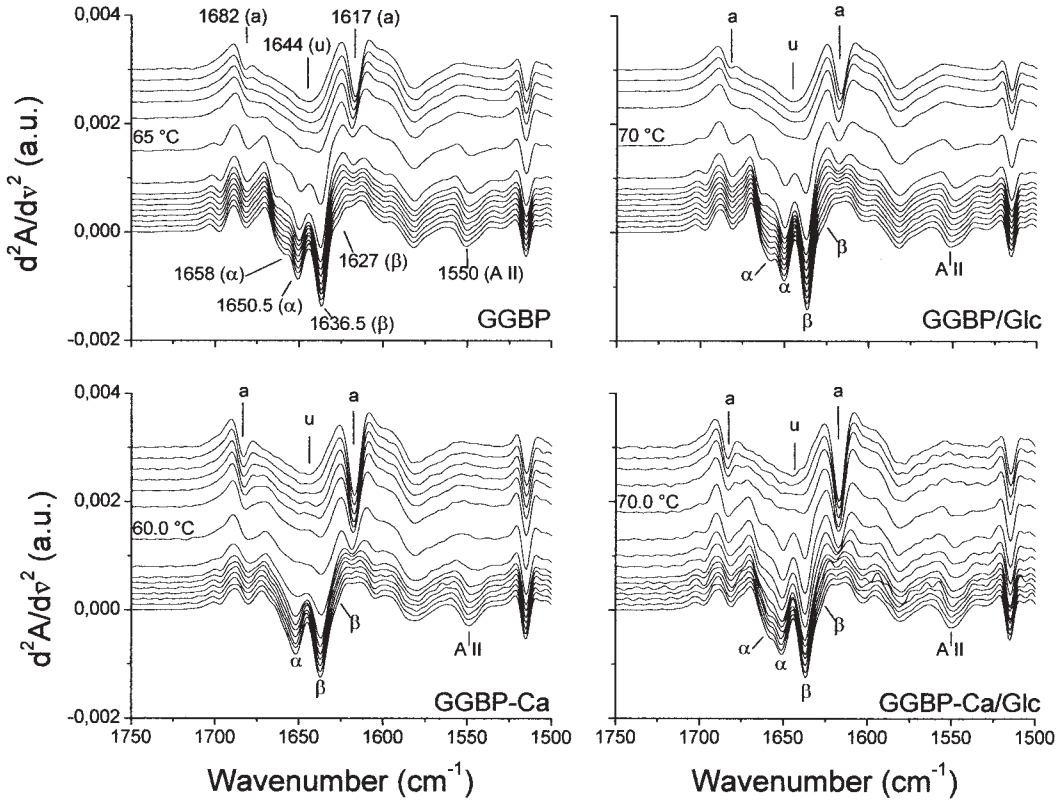

Fig. 5. **Second derivative spectra of GGBP, GGBP/Glc, GGBP-Ca and GGBP-Ca/Glc at different temperatures.** Spectra obtained between 20 and 90°C at 5°C increments. The letters (a) and (u) stand for aggregation and unordered structure, respectively. The symbols (α) and (β) stand for α-helix and β-sheet, respectively. The symbol (AII) refers to the residual amide II band.

and that they denature concomitantly, as shown by their T_m. However, it must be pointed out that in addition to the main α-helix and the main β-sheet bands, the spectra reported in Fig. 5 reveal the presence of other populations of β-sheets and α-helices that are particularly sensitive to high temperature, and that they disappear from the spectrum earlier to the T_m values reported in Table 2. All data suggest a sequence of events that may be summarized as follow: 1,627 cm^{-1} ↓, → 1,658 cm^{-1} ↓, → [1,636 cm^{-1} ↓, 1,651 cm^{-1} ↓], where the symbol (↓) indicates the decrease in intensity of the corresponding band. The sequence indicates that the first event is the decrease in intensity of the 1,627 cm^{-1} band, followed by the decrease in intensity of the 1,658 cm^{-1} band and by the concomitant decrease in intensity of the 1,636 cm^{-1} band and the 1,651 cm^{-1} band. The sequence is the same for all protein samples except for the GGBP-Ca sample whose spectrum does not display the 1,658 cm^{-1} band.

Molecular Dynamics Simulations—From the observation of the static 3D structure of the protein (Fig. 1A), it is evident that Ca^{2+} binds at the surface of the protein, and the residues that contact it belong essentially to a surface loop that it is assumed to be flexible. Thus, from this static structure it is hard to infer how high temperature can perturb the protein structure in both the presence of Ca^{2+} and after ion depletion. Therefore, in order to clarify the events occurring at a molecular level during the thermal destabilization of the GGBP and GGBP-Ca, two molecular dynamics simulations were performed by simulating the exposure of both GGBP and GGBP-Ca structures at 65°C. This temperature was chosen in order to maximize the conformational differences between the Ca^{2+}-depleted protein (T_m: 60.9°C) and the native one (T_m: 66.9°C). Since for the protein from *E. coli* (*35*) only crystallographic structures of the complexes with sugars (corresponding to the GGBP/Glc form) are available, we chose to conduct the computational analysis starting from the 3D structure of the protein from *S. typhimurium* in the presence of Ca^{2+} and in the absence of the sugar (corresponding to GGBP) (PDB ID code: 1GCG) (*5*) (Fig. 1A). This protein shares about 95% sequence identity to that from *E. coli*, and both the glucose and Ca^{2+}-binding sites are conserved between the two proteins, apart from the substitution of Gln 140, localized in the Ca^{2+} binding site of the *E. coli* protein, with Lys 140 in *S. typhimurium*. Thus, in our opinion, the results obtained using this system can be used as representative of the behaviour of GGBP from *E. coli*.

Figure 7 shows the results of molecular dynamics simulations. Panel A shows the mean conformation of GGBP-Ca after a 50 ps run, whereas in panel B the mean conformation of GGBP is reported. The RMSD between them is more than 3 Å, indicating that a large difference is present in the global conformation of the two systems after exposure to high temperatures. The differences are especially pronounced for the C-terminal

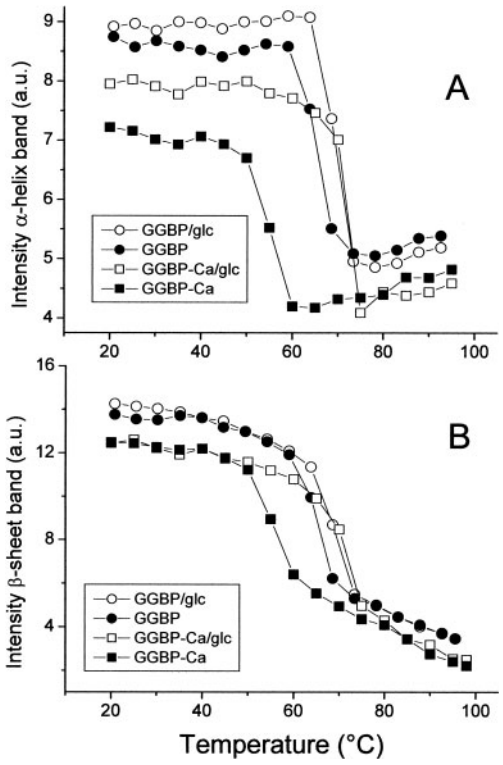

Fig. 6. **Temperature-dependent changes in the intensities of α-helix (A) and β-sheets bands (B) in GGBP, GGBP/Glc, GGBP-Ca and GGBP-Ca/Glc second derivative spectra.** The graphs were obtained by monitoring the intensity of the α-helix (1,650.5 cm^{-1}) and β-sheet (1,636.5 cm^{-1}) band intensities as a function of temperature.

Table 2. **Thermal denaturation of α-helix (1,650.5 cm^{-1}) and β-sheets (1,636.5 cm^{-1}) in GGBP, GGBP/Glc GGBP-Ca, and GGBP-Ca/Glc.**

Protein sample	Onset-α (°C)	Onset-β (°C)	T_m-α (°C)	T_m-β (°C)
GGBP	60	60	66.5	66.4
GGBP/Glc	65	65	70.6	70.1
GGBP-Ca	50	50	54.7	55.7
GGBP-Ca/Glc	65–70	65–70	71.7	71.6

Onset-α and Onset-β stand for the onset of temperature denaturation of α-helix (1,650.5 cm^{-1}) and β-sheets (1,636.5 cm^{-1}), respectively. T_m-α and T_m-β stand for the temperature of melting (T_m) of α-helix (1,650.5 cm^{-1}) and β-sheets (1,636.5 cm^{-1}), respectively.

domain, whereas the glucose binding site shows a quite limited difference between the two structures.

From the analysis of the mean conformation of GGBP-Ca after thermal denaturation (Fig. 7, panel A), it is evident that exposure to 65°C causes a large disruption in the secondary structures of GGBP-Ca, or at least a significant distortion of geometry that impairs recognition by the program DSSP. This is even more evident if the average structure obtained by molecular dynamics simulation is compared with the starting structure of the protein obtained by X-ray crystallography (see Fig. 1A). In particular, the β-sheet central to the C-terminal domain is almost completely missing, and only two β-strands are kept in proper position. Also In

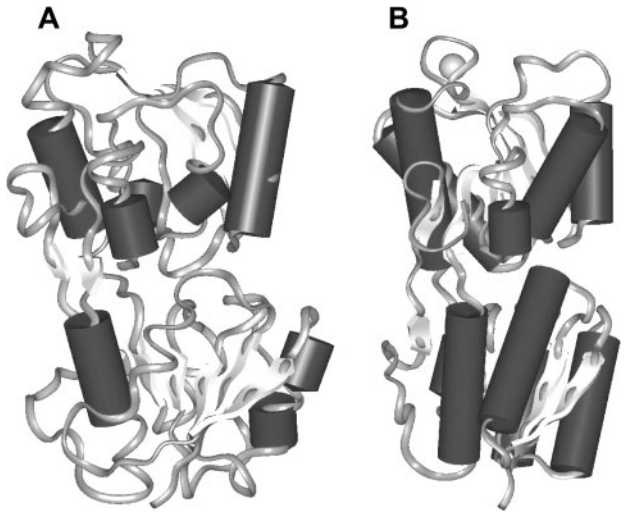

Fig. 7. **Molecular dynamics simulation results on GGBP from *S. typhimurium*.** (a) Average structure of GGBP-Ca obtained after 50 ps run at 65°C. (b) Average structure of GGBP obtained after 50 ps run at 65°C. Helices are represented as cylinders and β-sheets as arrows. The secondary structure elements were calculated with the program DSSP (see "MATERIALS AND METHODS").

this domain, the α-helices appear to be unfolded, except those in contact with the solvent and also the part of the helices that participate in sugar binding at the cleft between the N-terminal and the C-terminal domains. Also the N-terminal domain structure appears to be perturbed, but it is better conserved than the C-terminal domain. In fact, after the dynamics run, the central β-sheet appears to be almost intact, although the helices that surround it are largely missing.

These results are in agreement with the fluorescence and infrared data shown above, since the molecular portraits obtained by dynamics simulations confirm that the unfolding of the C-terminal domain of GGBP-Ca occurs with a lower T_m value with respect to the N-terminal domain (as inferred by fluorescence T_m compared with T_m by FT-IR), and that the unfolding of the GGBP-Ca protein is almost complete at 65°C, as deduced by the T_m from FT-IR data (Table 1). The average structure of GGBP in the presence of Ca^{2+} after exposure to a temperature of 65°C (Fig. 7, panel B) appears to be only slightly perturbed with respect to the starting structure obtained by X-ray crystallography (Fig. 1A). The overall fold of the protein is conserved and the structural elements are substantially present, with the exception of two α-helices in the C-terminal domain. This is also in agreement with the FT-IR data, since they show that the disappearance of secondary structural element bands occurs only above 70°C for GGBP. From the dynamics data it is evident that, although the metal ion is inserted in a binding site at the surface of the protein, it exerts a stabilizing effect that encompasses the whole structure of the protein, probably *via* the central β-sheet of the C-terminal domain. Ion depletion does not act only locally, but it also affects the core conformation of this domain that is no longer able to resist to the perturbation caused by the high temperature.

In conclusion, our data also show that the calcium depletion of GGBP markedly reduces the thermal stability of the protein, while it has a marginal effect on the presence of secondary structures at room temperature. The small changes in the secondary structure involve an α-helix band (1,658 cm^{-1}) that is not present in the calcium-depleted the GGBP spectrum, and that is restored in the GGBP-Ca/Glc spectrum. The nature of this band may be correlated with a population of α-helices or a segment of α-helix poorly exposed to the solvent. It is possible that the lack of the band in GGBP-Ca and its presence in GGBP-Ca/Glc is due to enhanced and reduced exposure to the solvent of the α-helix or part of it, respectively. The binding of glucose to GGBP-Ca also stabilizes the structure of the protein to high temperatures since the temperature of melting of GGBP-Ca/Glc was very similar to that of GGBP/Glc.

The reduced thermostability of GGBP-Ca documented by spectroscopic data is supported by molecular dynamics simulations showing that the calcium ion in GGBP exerts a stabilizing effect. Ca^{2+} depletion acts locally, but it also affects the conformation of the whole protein, and especially of the C-terminal domain that is markedly destabilized by high temperatures. In fact, our data underline that the perturbation in the structure of GGBP-Ca caused by high temperature involves the whole structure of the protein, but has a different impact on the two domains. The C-terminal domain is more affected by this perturbation, and it is largely disrupted; the N-terminal domain is also affected by high temperature, but its secondary and tertiary structures are better conserved, as it is evident from the comparison between Figs. 7A and 1A

Besides the basic knowledge, the new insights into GGBP constitute important data for the development of biotechnological applications requiring detailed information on the protein structural-functional properties as in the case of the manipulation of the protein to use as a probe for a biosensor of glucose monitoring.

We are grateful to Mr. Alan Weir for the language revision of the manuscript. This project was realized in the frame of CRdC-ATIBB POR UE-Campania Mis 3.16 activities (S.D., M.R) and the CNR commessa "Diagnostica avanzata ed alimentazione". This work was supported by grants from Università Politecnica delle Marche (F.T.), F.I.R.B. (S.D., M.R.), MIUR (S.D, M.R) and the Italian National Research Council (S.D, M.R).

REFERENCES

1. Ptitsyn, O.B. (1995) Molten globule and protein folding. *Adv. Protein Chem.* **47**, 83–229
2. Radford, S.E. (2000) Protein folding: progress made and promises ahead. *Trends Biochem. Sci.* **25**, 611–618
3. Vyas, N.K., Vyas, M.N., and Quiocho, F.A. (1987) A novel calcium binding site in the galactose-binding protein of bacterial transport and chemotaxis. *Nature* **327**, 635–638
4. Vyas, N.K., Vyas, M.N., and Quiocho, F.A. (1988) Sugar and signal-transducer binding sites of the *Escherichia coli* galactose chemoreceptor protein. *Science* **242**, 1290–12955.
5. Flocco, M.M. and Mowbray, S.L. (1994) The 1.9 Å X-ray structure of a closed unliganded form of the periplasmic glucose/galactose receptor from *Salmonella typhimurium*. *J. Biol. Chem.* **269**, 8931–8936
6. Zou, J.Y., Flocco, M.M., and Mowbray, S.L. (1993) The 1.7 Å refined X-ray structure of the periplasmic glucose/galactose receptor from *Salmonella typhimurium*. *J. Mol. Biol.* **233**, 739–752
7. Mowbray, S.L., Smith, R.D., and Cole, L.B. (1990) Structure of the periplasmic glucose/galactose receptor of *Salmonella typhimurium*. *Receptor* **1**, 41–53
8. Luck, L.A. and Falke, J.J. (1991) Open conformation of a substrate binding cleft: 19F NMR studies of cleft angle in the D-galactose chemosensory receptor. *Biochemistry* **30**, 6484–6490
9. D'Auria S. and Lakowicz, R.J. (2001) Enzyme fluorescence as a sensing tool: new perspectives in biotechnology. *Curr. Opin. Biotechnol.* **12**, 99–104
10. Salins, L.L., Ware, R.A., Ensor, C.M., and Daunert, S. (2001) A novel reagentless sensing system for measuring glucose based on the galactose/glucose-binding protein *Anal. Biochem.* **294**, 19–26
11. Staiano, M., Bazzicalupo, P., Rossi, M., and D'Auria, S. (2005) Advanced protein-based biosensors: Glucose biosensors as a model for analyses of high social interest. *Mol. BioSys.* **1**(5–6), 354–362
12. Staiano, M., Sapio, M.R., Scognamiglio,V., Marabotti, A., Facchiano, A.M., Bazzicalupo, P.M., Rossi, M., and D'Auria, S. (2004) A putative thermostable sugar-binding protein from the archaeon *Pyrococcus horikoshii* as a probe for the development of a fluorescence biosensor for diabetic patients. *Biotechnol. Progr.* **5**, 1572–1577
13. Notenboom, V., Boraston, A.B., Kilburn, D.G., and Rose, D.R. (2001) Crystal structures of the family 9 carbohydrate-binding module from *Thermotoga maritima* xylanase 10A in native and ligand-bound form. *Biochemistry* **40**, 6248–6256
14. Tolosa, L., Gryczynski, I., Eichhorn, L.R., Dattelbaum, J.D., Castellano, F.N., Rao, G., and Lakowicz, J.R. (1999) Glucose sensor for low-cost lifetime-based sensing using a genetically engineered protein. *Anal. Biochem.* **267**, 114–120
15. Piszczek, G., D'Auria, S., Staiano, M., Rossi, M., and Ginsburg, A. (2004) Conformational stability and domain coupling in D-glucose/D-galactose-binding protein from *Escherichia coli. Biochem. J.* **381**, 97–10316.
16. Bradford, M.M. (1976) A rapid and sensitive method for the quantitation of microgram quantities of protein utilizing the principle of protein-dye binding. Anal. Biochem. **72**, 248–254
17. Salomaa, P., Schaleger L.L., and Long, F.A. (1964) Solvent deuterium isotope effects on acid-base equilibria. *J. Am. Chem. Soc.* **86**, 1–7
18. D'Auria, S., Alfieri, F., Staiano, M., Palella, F., Rossi, M., Scirè, A., Tanfani, F., Bertoli, E., Grycznyski, Z., and Lakowicz, J.R. (2004) Structural and thermal stability characterization of *Escherichia coli* D-galactose/D-glucose-binding protein. *Biotechnol. Prog.* **20**, 330–337
19. Meersman, F., Smeller, L., and Heremans, K. (2002) Comparative Fourier transform infrared spectroscopy study of cold-, pressure-, and heat-induced unfolding and aggregation of myoglobin. *Biophys. J.* **82**, 2635–2644
20. Berman, H.M., Westbrook, J., Feng, Z., Gilliland, G. Bhat, T.N., Weissig, H., Shindyalov, I.N., and Bourne, P.E. (2000) The Protein Data Bank. *Nucleic Acids Res.* **28**, 235–242
21. Kabsch, W. and Sander, C. (1983) Dictionary of protein secondary structure: pattern recognition of hydrogen-bonded and geometrical features. *Biopolymers* **22**, 2577–2637
22. Arrondo, J.L., Muga, A., Castresana, J., and Goñi, F.M. (1993) Quantitative studies of the structure of proteins in solutions by Fourier-transform infrared spectroscopy. *Prog. Biophys. Mol. Biol.* **59**, 23–56
23. Tanfani, F., Lapathitis, G., Bertoli, E., and Kotyk, A. (1998) Structure of yeast plasma membrane H^+-ATPase: comparison of activated and basal-level enzyme forms. *Biochim. Biophys. Acta* **1369**, 109–118

24. Surewicz, W.K., Mantsch, H.H., and Chapman, D. (1993) Determination of protein secondary structure by Fourier transform infrared spectroscopy: A critical assessment. *Biochemistry* **32**, 389–394
25. Casal, H.L., Kohler U., and Mantsch, H.H., (1988) Structural and conformational changes of beta-lactoglobulin B: an infrared spectroscopic study of the effect of pH and temperature. *Biochim. Biophys. Acta* **957**, 11–20
26. Jackson, M. and Mantsch, H.H. (1991) Beware of proteins in DMSO. *Biochim. Biophys. Acta* **1078**, 231–235
27. Krimm, S. and Bandekar, J. (1986) Vibrational spectroscopy and conformation of peptides, polypeptides and proteins. *Adv. Protein Chem.* **38**, 181–364
28. Chirgadze, Y.N., Fedorov, O.V., and Trushina, N.P. (1975) Estimation of amino acid residue side-chain absorption in the infrared spectra of protein solutions in heavy water. *Biopolymers* **14**, 679–694
29. Barth, A. and Zscherp, C. (2002) What vibrations tell us about proteins. *Q. Rev. Biophys.* **35**, 369–430
30. Scirè, A., Saccucci, F., Bertoli, E., Cambria, M.T., Principato, G., D'Auria, S., and Tanfani, F. (2002) Effect of acidic phospholipids on the structural properties of recombinant cytosolic human glyoxalase II. *Proteins* **48**, 126–133
31. Ragusa, S., Cambria, M.T., Pierfederici, F., Scirè, A., Bertoli, E., Tanfani, F., and Cambria, A. (2002) Structure-activity relationship on fungal laccase from *Rigidoporus lignosus*: A Fourier-transform infrared spectroscopic study. *Biochim. Biophys. Acta* **1601**, 155–162
32. D'Auria, S., Barone, R., Rossi, M., Nucci, R., Barone, G., Fessas, D., Bertoli, E., and Tanfani, F. (1997) Effects of temperature and SDS on the structure of beta-glycosidase from the thermophilic archaeon *Sulfolobus solfataricus*. *Biochem. J.* **323**, 833–840
33. Pedone, E., Bartolucci, S., Rossi, M., Pierfederici, F.M., Scirè, A., Cacciamani, T., and Tanfani, F. (2003) Structural and thermal stability analysis of *Escherichia coli* and *Alicyclobacillus acidocaldarius* thioredoxin revealed a molten globule-like state in the thermal denaturation pathway of the proteins: An infrared spectroscopic study. *Biochem. J.* **373**, 875–883
34. Febbraio, F., Andolfo A., Tanfani, F., Briante, R., Gentile, F., Formisano, S., Vaccaro, C., Scirè, A., Bertoli, E., Pucci, P., and Nucci, R. (2004) Thermal stability and aggregation of *Sulfolobus solfataricus* beta-glycosidase are dependent upon the N-epsilon-methylation of specific lysyl residues: critical role of *in vivo* post-translational modifications. *J. Biol. Chem.* **279**, 10185–10194
35. Herman, P., Vecer, J., Barvik, I Jr.,Scognamiglio, V., Staiano, M., de Champodoré, M., Varriale, A., Rossi, M., and D'Auria, S. (2005) The role of calcium in the conformational dynamics and thermal stability of the D-galactose/D-glucose-binding protein from *Escherichia coli*. *Proteins* **61**, 184–195